

Influence of Transverse Deformation on Resonant Frequency of Patch Antenna

Kangqian Xu, Liyue Xie and Songtao Xue
*Research Institute of Structure Engineering
and Disaster Reduction
Tongji University
Shanghai, China
liyuxie@tongji.edu.cn*

Ke Xue and Guochun Wan
*Department of Electronic Science and Technology
Tongji University
Shanghai, China*

Abstract— The strain sensor based on microwave patch antenna is presented to monitor structural strain. Theoretically, the resonant frequency of antenna is determined by both the length and the width of the antenna. When the antenna is stretched uniaxially, the resonant frequency of the antenna shifts mainly due to its length change in longitudinal direction. However, the effect of the transverse deformation due to Poisson effect on resonant frequency of the antenna is yet to be confirmed and evaluated. Two sets of experiments are prepared to study the effect. The resonant frequencies of 2.45GHz chipless patch antennas with fixed length and varying width are tested; and the 920MHz chipped patch antennas are attached to the surface of specimens with the stretching direction parallel to length direction of antennas and perpendicular to length direction, respectively. Both types of specimens are stretched under different levels of tension force to determine the sensitivity coefficient between resonant frequency shift and antenna strain. Both results show that the influence of the transverse deformation of antennas on resonant frequency can be neglected, and its resonance frequency has a good linear relationship with the longitudinal strain.

Keywords—strain sensor, patch antenna, resonant frequency

I. INTRODUCTION

We are using the sensing technology extensively to collect valuable and reliable information about structures, including acceleration, displacement, strain and so on for safety assessment in structural health monitoring (SHM)^[1]. Among all these physical information, the strain can convey the incremental stress state of structural members locally.

The strain sensing technologies extensively used are metal foil strain gauges^[2], fiber optical sensors^[3] and so forth. Regardless its drift issue, the metal foil strain gauge is adopted widely because of its low cost, reliability and easy use. The fiber optical sensor detects the strain by the shift of the Bragg wavelength, but the sensor is vulnerable to damage when embedded in the structure. These conventional strain sensors need power lines and data cables for power supply and data transmission respectively, which makes sensor installation considerably labor- and time-consuming. And wired sensors could not acquire data due to power failure or cable malfunction during extreme disasters.

Trying to get rid of cables entirely in the sensing system, the wireless sensors are developed and applied to ease the

sensor installation and data transmission^[4, 5]. Energy harvest technologies (battery, solar energy, vibration) are utilized to eliminate power cables. However, the sensor still need active and consistent power supply when collecting information, which makes the solution half the way towards the destination.

It is found and confirmed that the resonant frequency of the antenna will shift mainly due to its deformation. This phenomenon can make the antenna as a sensing unit for strain (deformation) by converting the mechanical strain into electrical signals. The mechanical strain can be detected and the electrical signals are transmitted to the reader via the technology of radiofrequency identification (RFID)^[6, 7] simultaneously. Yi et al.^[8, 9] developed the smart-skin folded patch antenna sensor. The resonant frequency of patch antenna can be identified easily due to its narrow bandwidth and it shifts almost linearly with antenna's deformation. Due to dual function of passive sensing and wireless communication, various antenna sensors have been developed for evaluating structural health state^[10, 11], and recent work demonstrates the great potential for the application in SHM.

Strain sensors are required to detect deformation in structures accurately and reliably. Among all issues, sensitivity of antenna sensors to deformation is one of the greatest concerns. However, the two aspects affecting the measured sensitivity: (i) the efficiency of mechanical strain transfer from the base structure to the top surface of the RFID antenna sensor; (ii) the unintentional influence of transverse deformation other than the measured direction on the resonant frequency of the antenna. When the antenna is stretched uniaxially, the resonant frequency of the antenna shifts mainly due to its length change in longitudinal direction. However, the effect of the transverse deformation due to Poisson effect on resonant frequency of the antenna is yet to be confirmed and evaluated.

In this paper, in order to investigate the influence of transverse deformation on the resonant frequency of the patch antenna, two sets of patch antennas at different operating frequencies are prepared: 2.45GHz chipless patch antennas with fixed length and varying width, the 920MHz chipped patch antennas. And two kinds of experiments are designed to obtain different transverse deformations under the same longitudinal deformations of antennas. The first approach is that the patch antennas with fixed length and varying width are stretched and the other approach is that the patch antennas

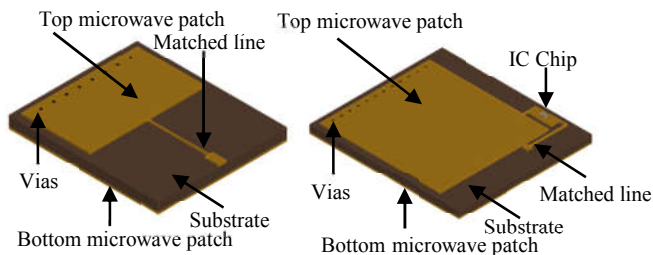
attached to the specimens longitudinally and transversely respectively are stretched. In addition to the approaches mentioned above, biaxial stretching experiment seems a better choice to explore the influence of transverse deformation on resonant frequency of antennas by keeping the longitudinal length of antennas and applying the width deformation to the antennas. But the additional equipment increases the cost of experiment. So the approaches in this paper are easier to implement compared with others.

The rest of the paper is organized as follows. In the Section II, the design principle of the two kinds of patch antennas and measurement mechanism of resonant frequency are briefly introduced. The Section III presents the tensile experiments of 2.45GHz chipless patch antennas with fixed length and varying width, and analyzes the results of experiments. The Section IV presents the design and analysis of the experiments of 920MHz chipped patch antennas which are attached to aluminum plates longitudinally and transversely respectively. The Section V provides a summary and discussion of this work.

II. STRAIN SENSING SYSTEM

We design two sets of strain sensors based on quarter-wavelength rectangular patch antennas to explore the influence of transverse deformation on resonant frequency of antenna. One set is chipped antenna sensors with resonant frequencies around 920MHz (Fig. 1(a)) and the other is chipless antenna sensors with resonant frequencies around 2.45GHz (Fig. 1(b)). Both strain sensors are composed of top microwave patch, bottom microwave patch, vias, substrate and matched line, as illustrated in Fig. 1. The only difference between these two sets is the IC chip integrated with the 920MHz antennas. As a part of the strain sensor, the IC chip can harvest the electromagnetic wave emitted by RFID readers, and send the information stored in chips back to readers. In this way, the 920MHz chipped strain sensors can be interrogated by the readers wirelessly without any power supply.

On the other hand, since the RFID IC chip operating around 2.45GHz is not available in the market, we design the 2.45GHz strain sensor without IC chips. In order to measure the resonant frequency's shift, the coaxial cable is connected with the matched line to send electromagnetic waves into the antennas and receive the reflected electromagnetic waves.



(a) 2.45GHz Chipless antenna sensor (b) 920MHz Chipped antenna sensor
Fig. 1. Two sets of patch antenna sensors

A. Design Principle of Antennas

For a quarter-wavelength rectangular patch antenna, the initial resonant frequency f_{R0} can be estimated by the following equation^[12]

$$f_{R0} = \frac{c}{4(L_1 + 2\Delta L_1)\sqrt{\epsilon_e}} \quad (1)$$

where c is the speed of light, L_1 is the length of the top microwave patch, ϵ_e is the effective dielectric constant of the substrate, and ΔL_1 is the additional dielectric length considering edge-fringing field. The effective dielectric constant ϵ_e can't be measured directly and it is related to relative dielectric constant ϵ_r of the substrate^[12]:

$$\epsilon_e = \frac{\epsilon_r + 1}{2} + \frac{\epsilon_r - 1}{2} \left(1 + \frac{10H}{W_1}\right)^{-\frac{1}{2}} \quad (2)$$

where H is the substrate thickness and W_1 is the width of the top microwave patch.

The compensating additional dielectric length is defined as^[12]:

$$\Delta L_1 = 0.412H \frac{(\epsilon_e + 0.3)(W_1/H + 0.264)}{(\epsilon_e - 0.258)(W_1/H + 0.8)} \quad (3)$$

When the antenna experiences strain deformation of ϵ , the length of the top microwave patch becomes $L_1(1+\epsilon)$ in the longitudinal direction, and the width and thickness become $W_1(1-\nu\epsilon)$ and $H(1-\nu\epsilon)$ in the transverse direction, respectively, where ν is the Poisson's ratio of the substrate. The resonant frequency f_R under strain of ϵ can be calculated by the following equation:

$$f_R = \frac{c}{4(L_1(1+\epsilon) + 2\Delta L_1(1-\nu\epsilon))\sqrt{\epsilon_e}} \quad (4)$$

The additional dielectric length ΔL_1 is significantly smaller than the length of the patch L_1 . Therefore, the resonant frequency f_R of a quarter-wavelength rectangular patch antenna can be simplified by ignoring ΔL_1 , and (4) becomes:

$$f_R \approx \frac{c}{4\sqrt{\epsilon_e} L_1(1+\epsilon)} = \frac{f_{R0}}{1+\epsilon} \approx f_{R0}(1-\epsilon) \quad (5)$$

Equation (5) shows that the resonant frequencies of antennas depend linearly on the strain that the antennas experience, if we ignore the influence of the substrate's transverse deformation on the antenna's resonant frequency.

B. Measurement of Resonant Frequency of 2.45GHz Antenna

The antenna receives the interrogating electromagnetic signal from the reader and transmits it to the circuit load of the strain sensor. However, a portion of the input waves is reflected by the antenna, thus this portion of energy will be wasted. The ratio of the reflected power to the input power is described as reflection coefficient $\eta(f)$ ^[13]:

$$\eta(f) = \frac{P^-}{P^+} = \left| \frac{Z_L - Z_0^*}{Z_L + Z_0} \right|^2 \quad (6)$$

where P^+ is the input power, P^- is the reflected power, Z_L is the load impedance, Z_0 is the impedance of the patch antenna, Z_0^* is the conjugate of the Z_0 , which is a function of the antenna's operating frequency. When the antenna operates at its resonant frequency, the impedance of the antenna matches the circuit load the best and the least energy will be reflected by the antenna.

For a 2.45GHz chipless patch antenna, the return loss curve can be measured by a vector network analyzer (VNA) as shown in Fig. 2. The return loss coefficient S_{11} is measured at each frequency within a certain range, which is defined as^[13]:

$$S_{11} = 10 \lg \eta(f) \quad (7)$$

The same as reflection coefficient $\eta(f)$, the return loss coefficient reaches minimum at the resonant frequency of the antenna, so that the resonant frequency can be extracted easily from the return loss curve.

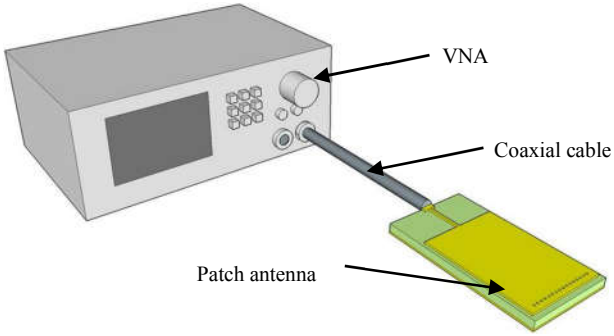


Fig. 2. Measurement of resonant frequency of antenna by VNA

C. Measurement of Resonant Frequency of 920MHz Antenna

The wireless sensing system of the 920MHz patch antenna sensor is shown in Fig. 3. In this system, the antenna sensor receives the electromagnetic signal emitted by the reader, and reflects the signal back to the reader with the power P_1' , which can be estimated according to Friis free space formula^[14]:

$$P_1' = P_2' G_1 G_2 \left(\frac{\lambda}{4\pi d} \right)^2 = P_2' G_1 G_2 \left(\frac{c}{4\pi d f} \right)^2 \quad (8)$$

where P_1' is the reflected power, P_2' is the transmitted power of patch antenna, G_1 is the reader antenna gain, G_2 is the patch antenna gain, λ is the wavelength of the electromagnetic wave emitted by the reader, d is the distance between the reader and the patch antenna, and f is the frequency of the interrogation wave.

Inside the antenna sensor, the power is transferred from the patch antenna to the load and back to the patch antenna again with the power P_2' , which can be obtained by the following equation:

$$P_2' = P_3 (1 - \eta(f)) \quad (9)$$

where P_3 is the power of the IC chip, $\eta(f)$ is the same as the reflection coefficient defined in (6). As the load of the antenna, the IC chip will be activated when the power is higher than the power threshold P_{IC} . Substituting (9) into (8), the reflected power threshold P_{1S}' , can be calculated as:

$$P_{1S}' = P_{IC} G_1 G_2 \left(\frac{c}{4\pi d} \right)^2 \frac{(1 - \eta(f))}{f^2} \quad (10)$$

According to the property of function $\eta(f)$, the reflected power threshold curve reaches the maximum when the interrogation frequency is equal to the resonant frequency of the patch antenna.

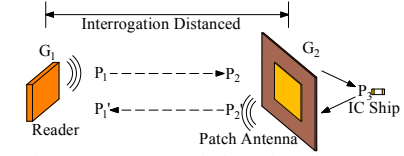


Fig. 3. Power transmission of sensing system

III. TEST OF 2.45GHz CHIPLESS PATCH ANTENNA

In order to study the effect of the transverse deformation on resonant frequency of the antenna, two types of 2.45GHz patch antennas with fixed length and varying width are designed. By tension experiments, the sensitivity coefficient between resonant frequency shift and antenna strain of different levels are evaluated.

A. Experiment Design

The dimension of 2.45GHz patch antennas in Fig. 4 are designed according to (1), (2) and (3). The parameters and dimensions of antennas are listed in TABLE I and II, the wide patch antenna has a width with 35mm and the narrow one is 17mm wide. When the strain of the wide patch antenna changes from 0 to 10000 $\mu\epsilon$, the resonant frequencies calculated by (4) and (5) are shown in Fig. 5(a). The relative error increases as the strain increases, and it arrives 0.046% when strain becomes 1%, which is acceptable in engineering.

Tension experiments of the 2.45GHz antenna sensors are conducted. The wide and narrow patch antennas are bonded on aluminum specimens for stretching, respectively, as shown in Fig. 6. Prescribed loads are applied at the two ends of specimen from 0 to 12kN, so that different strain levels (from 0 to 700 $\mu\epsilon$ approximately) can be generated in the specimen.

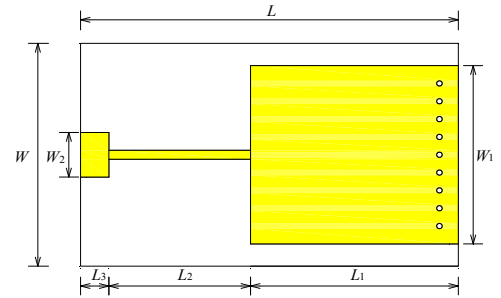


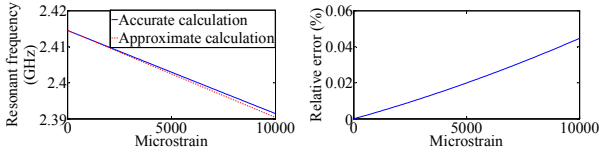
Fig. 4. The parameters of 2.45GHz patch antenna

TABLE I. THE DIMENSIONS OF THE WIDE PATCH ANTENNA

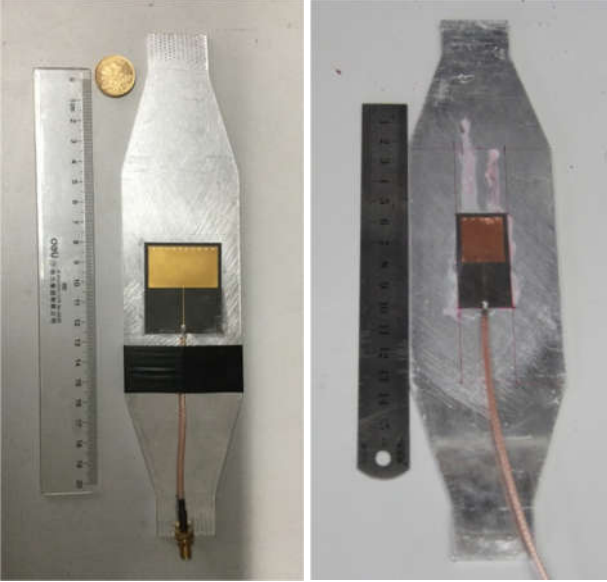
Parameters	W	L	H	W_1	W_2	L_1	L_2	L_3
Dimensions(mm)	39	45.4	0.5	35	2.1	20.6	18.7	4

TABLE II. THE DIMENSIONS OF THE NARROW PATCH ANTENNA

Parameters	W	L	H	W_1	W_2	L_1	L_2	L_3
Dimensions(mm)	21	45.4	0.5	17	2.1	20.6	18.7	4



(a) Strain-resonant frequency calculated curves (b) Relative error
Fig. 5. The comparison of strain-resonant frequency curves



(a) The wide antenna specimen (b) The narrow antenna specimen
Fig. 6. Experimental specimens of 2.45GHz patch antenna

B. Analysis of Test Results

At each strain level, the return loss curve is obtained by VNA and the resonant frequency of antennas is extracted from the curve by picking the minimum point with least reflected energy. Then the resonant frequency shift is fitted with respect to the applied strain by linear regression method, as shown in Fig. 7 and TABLE III.

The measured initial resonant frequencies of the wide and narrow antennas are 2.522GHz and 2.452GHz respectively. And the slopes of the fitted lines, which represent the sensitivity coefficients of antenna sensors, are $-1.777\text{GHz}/\varepsilon$ for wide antennas and $-1.793\text{GHz}/\varepsilon$ for narrow ones, respectively. Comparison between these two antennas is made using the ratios of the sensitivity coefficients to initial resonant frequencies. The relative error between the two ratios, 0.705 and 0.731, is 3.69%. Considering the transfer efficiency of the narrow antenna is slightly higher than that of the wide antenna, the influence of the transverse deformation on the resonant frequency can be neglected for the 2.45GHz patch antenna within the tolerable error.

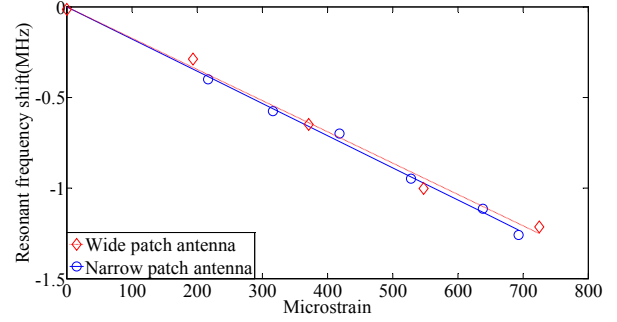


Fig. 7. Strain-resonant frequency fitted lines

TABLE III. THE TEST RESULTS OF THE 2.45GHz PATCH ANTENNA

Sample	The initial resonant frequency (GHz)	The slope of fitted line (GHz/ ε)	The ratio
Wide patch antenna	2.522	1.777	0.705
Narrow patch antenna	2.452	1.793	0.731

IV. TEST OF 920MHZ CHIPPED PATCH ANTENNA

We attach the chipped antenna sensors onto the surface of specimens in two ways. The length direction of antennas is parallel to the tension direction that the antennas suffer (longitudinally pasted antenna); the other situation is that the width direction of antennas is in the line with the tension direction (transversely pasted antenna). Considering the efficiency of mechanical strain transfer from the base structure to the top surface of the antenna sensor, defined as η , the longitudinal strain of the top surface of the antenna is $\eta\varepsilon$ and the transverse strain of the top surface is $\nu\eta\varepsilon$, when the stretched specimen has a strain of ε for the case of longitudinally pasted antenna. For the case of transversely pasted antenna, the longitudinal strain of the top surface of the antenna is $\nu\eta\varepsilon$ and the transverse strain of the top surface is $\eta\varepsilon$. In the two cases, the ratios of longitudinal deformation to transverse deformation of antennas, $1/\nu$ and ν respectively, are different. In other words, when the longitudinal deformation of longitudinally pasted antenna is the same as transversely pasted antenna, the transverse deformations of them are inconsistent. So the influence of transverse deformation on the resonant frequency of the patch antenna can be verified by comparing the ratio of the two slopes of fitted strain-resonant frequency lines with the Poisson's ratio ν .

A. Experiment Design

The dimensions of the 920MHz patch antenna are shown in Fig. 8 and TABLE IV. The patch antennas are longitudinally and transversely attached to the center of the specimens for tension experiments, and the two kinds of specimens are shown in Fig. 9.

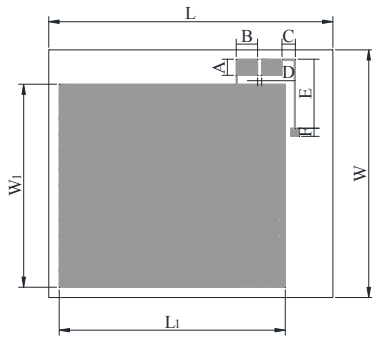
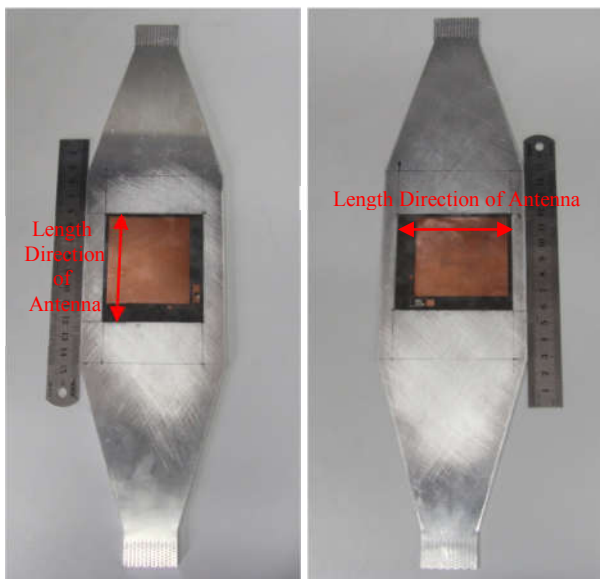


Fig. 8. The parameters of 920MHz patch antenna

TABLE IV. 920MHZ PATCH ANTENNA SPECIFIC DIMENSIONS

Parameters	L	W	L_1	W_1	A	B	C	D	E	F
Dimensions(mm)	69	61	54.9	50	3.96	4.93	3	1.02	18	2.5



(a) Longitudinally pasted antenna (b) Transversely pasted antenna
Fig. 9. The two kinds of experimental samples

B. Analysis of Test Results

At every load step sending the interrogation signals with frequency ranging around the initial resonant frequency, the reflected power threshold curve of the antenna is obtained by measuring the reflected power. And the reflected power threshold curve reaches its maximum at the resonant frequency. After we get all the resonant frequencies of antennas for every strain steps, the linear regression method is used to fit the data between the antenna strain and the resonant frequency, which is shown in Fig. 10 and TABLE V.

The initial resonant frequencies of the same kind of antennas may differ a bit due to the manufacturing error. Likewise, the ratio of the slope to initial resonant frequency is also used to explain the effect of transverse deformation on electromagnetic characteristics. The average value of the ratio is 0.761 when antennas are pasted longitudinally and it is 0.306 when antennas are pasted transversely. The ratio between these two cases is 0.402, whose relative error is only 0.5% to the

Poisson's ratio 0.4 of the substrate made of RT/duroid[®]5880. Therefore, the influence of the transverse deformation on resonant frequency is negligible in engineering.

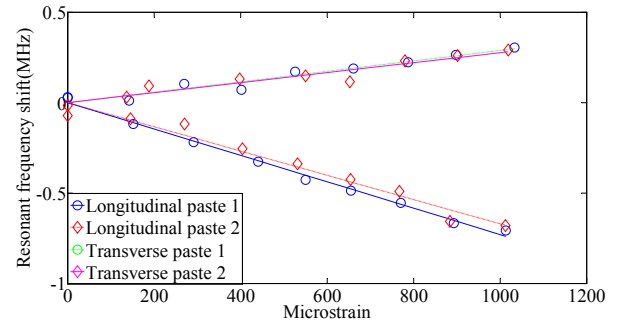


Fig. 10. Strain-resonant frequency shift curves

TABLE V. THE TEST RESULTS OF THE 920MHZ PATCH ANTENNA

Sample	The initial resonant frequency (MHz)	The slope of fitted line (MHz/ ϵ)	The ratio	Average
Longitudinal pasted 1	922.03	729.89	0.792	0.761
Longitudinal pasted 2	918.97	670.33	0.729	
Transverse pasted 1	918.66	288.03	0.314	0.306
Transverse pasted 2	921.62	275.90	0.299	

V. CONCLUSION

Strain sensors with rectangular patch antennas are proposed for detecting the incremental strain in structural members. In this paper, we designed two sets of strain sensors to study the influence of the transverse deformation on the resonant frequencies of antennas: the 2.45GHz chipless patch antennas with fixed length and varying width are tested and the 920MHz chipped patch antennas. Both types of sensors are stretched under tension forces to determine the sensitivity coefficient between the resonant frequency shift and the antenna strain. Sensors with chipless patch antennas are wired by VNA for detecting the return loss curve; sensors with chipped ones can be interrogated wirelessly by a reader for acquiring the reflected power threshold curve.

The resonance frequencies of both sensors have a nice linear relationship with the experienced strain of the antennas. Chipless patch antennas with different width have close sensitivity coefficients with tolerable difference. And the ratio between sensitivity coefficients of chipped patch antennas longitudinally and transversely glued on the specimens is also very close to the Poisson's ratio 0.4 of the substrate. These results verified that the influence of the transverse deformation on antenna's resonant frequency is negligible and the proposed strain sensors can be adopted for measuring the strain in interested direction without considering the minor effect induced by transverse deformation of the base material.

ACKNOWLEDGMENT

This study was supported by the National Natural Science Foundation of China (Grant No.51478356), the Key Program of intergovernmental international scientific and technological innovation cooperation (Grant No. 2016YFE0127600), and by the Fundamental Research Funds for the Central Universities.

REFERENCES

- [1] Sohn H, Farrar C R, Hemez F M, et al. A Review of Structural Health Monitoring Literature: 1996 - 2001[J]. *Data Acquisition*, 2004,1a-13976-m.
- [2] Wisniewski Z, Wisniewski R, Nowinski J L. Application of foil strain gauges in high pressure research[J]. *Review of Scientific Instruments*, 2001,72(6):2829-2831.
- [3] Zhou Y, So R M C, Jin W, et al. Dynamic strain measurements of a circular cylinder in a cross flow using a fibre Bragg grating sensor[J]. *Experiments in Fluids*, 1999,27(4):359-367.
- [4] Kurata N, Jr B F S, Ruiz-Sandoval M. Risk monitoring of buildings with wireless sensor networks[J]. *Structural Control & Health Monitoring*, 2010,12(3-4):315-327.
- [5] Liu L, Yuan F G. Wireless sensors with dual-controller architecture for active diagnosis in structural health monitoring[J]. *Smart Material Structures*, 2008,17(2):2900-2912.
- [6] Rao K V S, Nikitin P V, Lam S F. Antenna design for UHF RFID tags: a review and a practical application[J]. *IEEE Transactions on Antennas & Propagation*, 2005,53(12):3870-3876.
- [7] Li S, Visich J K, Khumawala B M, et al. Radio frequency identification technology: applications, technical challenges and strategies[J]. *Sensor Review*, 2006,26(3):193-202.
- [8] Xiaohua Y, Terence W, Yang W, et al. Passive wireless smart-skin sensor using RFID-based folded patch antennas[J]. *International Journal of Smart & Nano Materials*, 2011,2(1):22-38.
- [9] Yi X, Wu T, Wang Y, et al. Sensitivity Modeling of an RFID-Based Strain-Sensing Antenna With Dielectric Constant Change[J]. *IEEE Sensors Journal*, 2015,15(11):6147-6155.
- [10] Xu X, Huang H. Battery-less wireless interrogation of microstrip patch antenna for strain sensing[J]. *Smart Materials & Structures*, 2012,21(12):125007.
- [11] Cho C, Yi X, Li D, et al. Passive Wireless Frequency Doubling Antenna Sensor for Strain and Crack Sensing[J]. *IEEE Sensors Journal*, 2016,16(14):5725-5733.
- [12] Finkenzeller K. *RFID Handbook: Fundamentals and Applications in Contactless Smart Cards and Identification*, Second Edition[M]. John Wiley & Sons Ltd, 2003.
- [13] Stutzman W L, Thiele G A. *Antenna theory and design*[J]. *Electronics & Power*, 1981,28(3):267.
- [14] Balanis C A. *Antenna Theory: Analysis and Design*[M]. Harper & Row, 1982.